Available online at www.sciencedirect.com

ScienceDirect

Procedia Engineering 139 (2016) 15 – 21

Procedia Engineering

www.elsevier.com/locate/procedia

MRS Singapore – ICMAT Symposia Proceedings

8th International Conference on Materials for Advanced Technologies

Bismuth ferrite enhanced ZnO solid state dye-sensitised solar cell

Leonard Loh[a,b], Joe Briscoe[a] and Steve Dunn,[*a]

[a]Queen Mary, University of London, Mile End Road, London E1 4NS, UK

[b]Nanyang Polytechnic, 180 Ang Mo Kio Avenue 8, S809687, Singapore

Abstract

ZnO dye sensitized solar cells have been reported to be plagued with issues of dye aggregation which increased current recombination. This dye aggregation has been linked to the pH 5 ruthenium-based dye solutions, which is below ZnO's point of zero charge of pH 9, resulting in positive surface charges on ZnO which form Zn2+ - dye complexes. In this paper, a heterogeneous architecture of ZnO and bismuth ferrite (BiFeO3 or BFO) is synthesized using a technique which allows the synthesis using purely chemical solution techniques. BFO is a perovskite studied extensively for its multiferroic properties and its potential for anomalous photovoltages. The solid state solar cells are sensitized with N719, and uses copper thiocyanate (CuSCN) as a hole conductor. The ZnO-BFO-N719-CuSCN heterogeneous architecture solar cell showed efficiencies which increased ca four-fold to 0.38% and Jsc which doubled to 1.38 mA/cm2 compared to ZnO-N719-CuSCN architectures. We will report that the addition of BFO improved performances due to the reduction of dye aggregation due to BFO's pzc of pH 6.5 which is close to the pH 5 of the dye solution, as well as BFO's role as an electron blocking layer which prevents the back tunneling of electrons from ZnO to CuSCN.

Selection and/or peer-review under responsibility of the scientific committee of Symposium 2015 ICMAT

Keywords: ZnO; $BiFeO_3$; solar; CuSCN

1. Introduction

The use of ZnO in DSSCs has gained momentum in the last 15 years due to its high electron mobility and electron diffusion coefficient.[1] In the last 5 years, the use of perovskites, in particular the organo-lead halides, as sensitizers in combination with spiro-OMeTAD hole conductors, have boosted the performances of DSSCs significantly, achieving efficiencies over 20%.[2,3] One of the perovskites that have been reported to exhibit photovoltaic properties is bismuth ferrite, $BiFeO_3$ (BFO).[1,4] BFO has matching energy bands to ZnO, which

Selection and/or peer-review under responsibility of the scientific committee of Symposium 2015 ICMAT

doi:10.1016/j.proeng.2015.09.235

makes BFO a strong candidate for developing heterogenous structures with ZnO. To be able to deposit BFO effectively over high aspect ratio ZnO nanostructures like nanorods, presents a challenge for uniform and effective coating when using vacuum-based processes. The most effective method would be to use chemical solution techniques. However, one of the issues faced by ZnO is the poor chemical stability in corrosive environments.[5] As chemical solution deposited BFO uses solutions with pH below pH 1, the deposition of BFO on ZnO would react with or dissolve ZnO. This paper reports a technique which allows the chemical solution deposition of BFO on ZnO through the use of self-assembled monolayers, 3-aminopropyltriethoxysilane, $H_2N(CH_2)_3Si(OC_2H_5)_3$ (APTES), as a protective medium. Solid state solar cells with heterogeneous ZnO-BFO structures, sensitized with N719 with CuSCN hole conductor were fabricated and the performance were evaluated and compared with ZnO-N719-CuSCN devices.

2. Experimental

Materials Synthesis: Seeding was done on 15 Ω fluorine-doped tin oxide (FTO) coated glass substrates by dropping 5 mM of absolute ethanolic zinc acetate ($Zn(CH_3CO_2)_2$) on the conductive face of the substrate and rinsing with ethanol. The process was repeated 15 times with 3 intermediate annealing steps at 350 °C for 25 min on a hotplate. The ZnO nanorods were then synthesized by suspending the seeded substrates in 25 mM zinc nitrate ($Zn(NO_3)_2.6H_2O$) and 25mM of hexamethylenetetramine or HMT ($C_6H_{12}N_4$) in deionised (DI) water at 90 °C for 15 hours, with a change of precursor solution every 2.5 hours.[6] The ZnO nanorods were soaked in a solution of 4% APTES in toluene at 60 °C for 30 minutes before rinsing with toluene. Samples were heated to 90 °C for an hour to remove excess solvents and allow curing of the APTES. 0.075 M to 0.3 M BFO precursor sol concentrations were prepared using bismuth nitrate pentahydrate ($Bi(NO_3)_3.5H_2O$) and iron nitrate nonahydrate ($Fe(NO_3)_3.9H_2O$) mixed in 2-methoxyethanol ($CH_3OCH_2CH_2OH$) solvent. To control the viscosity and gelation time, 2 % by volume of ethanolamine ($NH_2(CH_2)_2OH$) and 20% by volume of the dehydrating agent, acetic anhydride ($(CH_3CO)_2O$) was added. The BFO sol was deposited by spin coating at 2000 rpm for 10 seconds followed by 5000 rpm for additional 20 seconds. The gelation was activated by first preannealing at 100 °C for 1 minute to stabilize the film, followed by 350 °C for 3 minutes on a hot plate. Annealing at 600 °C for 2 hours in air in a furnace fully crystallized the BFO films. All chemicals used were Sigma Aldrich analytical grade reagents unless otherwise stated.

Solar Cell Device Fabrication: The active layer was first coated with 0.5 mM of a dye sensitizer, N719 from Dyesol for 15 hours, followed by rinsing with absolute ethanol to remove excess dye. Dupont's 25 µm Surlyn film was used as a spacer and as an insulating layer outside the active area. CuSCN was used as a hole conducting medium. 0.2 M CuSCN in dipropyl sulfide solvent was micro-sprayed onto 90 °C heated samples using an Iwata airbrush system.[7,8] 150 nm thick Au counter electrodes were sputtered using the Denton Vacuum Explorer 14 thermal evaporator with a power of 125 W, base pressure of 4×10^{-2} mTorr and working pressure of 100 mTorr at an ambient temperature in 100% Argon atmosphere.

Characterisation: All morphology, cross-section and surfaces of the films, crystallographic information as well as elemental analysis of the films surface were performed using the Jeol JSM 6701F field emission scanning electron microscope (FESEM) and Jeol JEM2100 transmission electron microscope (TEM). Optical absorbance spectra were measured using the Perkin Elmer Lambda 950 UV visible spectroscopy. Dye loading studies were conducted by extracting the dyes through soaking for 12 hours in 5 ml of 0.1 M NaOH in ethanol/water (volume 1:1). The diffraction peaks of the films were studied using the Panalytical X'pert Pro X-ray diffraction (XRD) with CuK_α 1 radiation at k = 1.54056 Å. Hall mobility measurements were conducted using the Van der Pauw method at room temperature from an average of 10 measurements with a compliance voltage of 5 V, measurement current of 50 µA, magnetic field of 0.5 T for a dwell time of 1 second. The current density (J) – voltage (V) relationships were tested with the IVT Solar VS 6820 solar simulator system with a Keithley 2400 source meter under 100 mW/cm^2, AM 1.5G simulated sunlight. The incident photon-current conversion efficiency (IPCE) of some N719 sensitized solar cells were measured using the IVT Solar VS 6851 system at room temperature with an incident light ranging from 350 to 800 nm with a sampling rate of 5 nm per second.

3. Results and discussion

3.1. Materials Synthesis

The synthesized ZnO nanorods are shown in Fig. 1, where an average diameter and length of 120 nm and 2.6 µm was obtained. The XRD data gave a wurztite crystallinity with a strong dominant (0002) crystal plane. The band gap for the ZnO nanorods was *ca* 3.3 eV estimated from the Tauc plot.

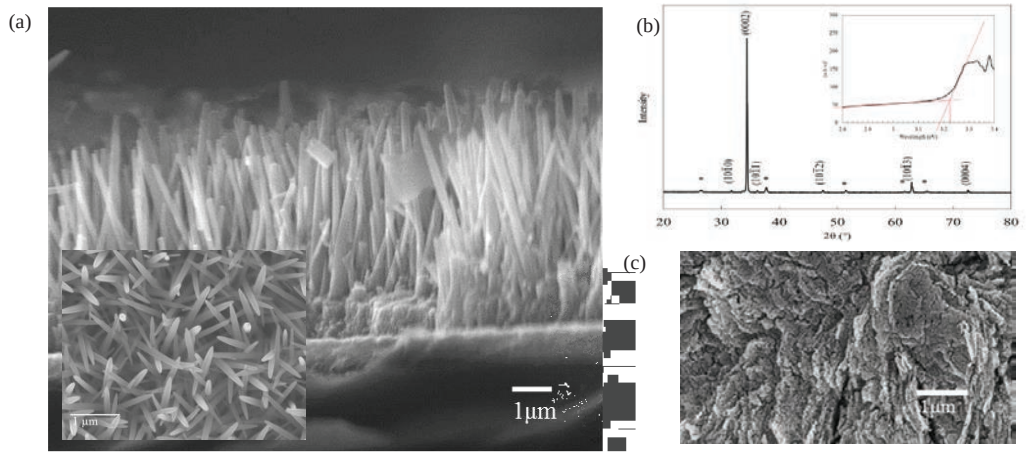

Fig. 1. (a) Cross-section of ZnO nanorods synthesized using equimolar of 25 mM for $Zn(NO_3)_2$ and HMT for 15 hours (inset shows top view) , (b) XRD of ZnO nanorods (inset shows Tauc plot), (c) chemical dissolution of ZnO by BFO sol[9]

One of the disadvantages of ZnO is its chemical stability in corrosive environments. When 0.3 M BFO sol was spin-coated onto the ZnO nanorods, rapid dissolution occurred (Fig. 1(c)). ZnO dissolution has been reported to occur rapidly when exposed to environments with pH < 4.[10] The pH of the various concentrations of BFO are shown in Table 1, which were all below pH 3. This explains the rapid dissolution of the ZnO when BFO was spin-coated.

Table 1. pH of various BFO concentration

Concentration of BFO sol (M)	pH
0.3	0.6
0.15	0.8
0.075	2.75

The APTES layer dip-coated onto the ZnO nanorods before spin-coating the BFO, acted as a buffer layer which protected the ZnO, preventing dissolution.[11] The morphology of the BFO coating using various concentrations of BFO sol to generate different BFO coating thicknesses is shown in Fig. 2. When 0.075 M of BFO was used, the BFO coating was patchy with islands of BFO coverage, resulting in exposed ZnO nanorods. The selected area electron diffraction pattern (SAED) data showed both the presence of ZnO (0002) and BFO (110) crystal phases. Increasing the BFO sol concentration to 0.15 M gave conformal coating of the ZnO nanorods (Fig. 2(c)) with a thickness of *ca* 2.5 nm. The SAED data showed BFO (110) and BFO (104) crystallinity. Increasing the concentration of the BFO sol increased the thickness further with a thickness ranging from *ca* 7 – 20 nm.

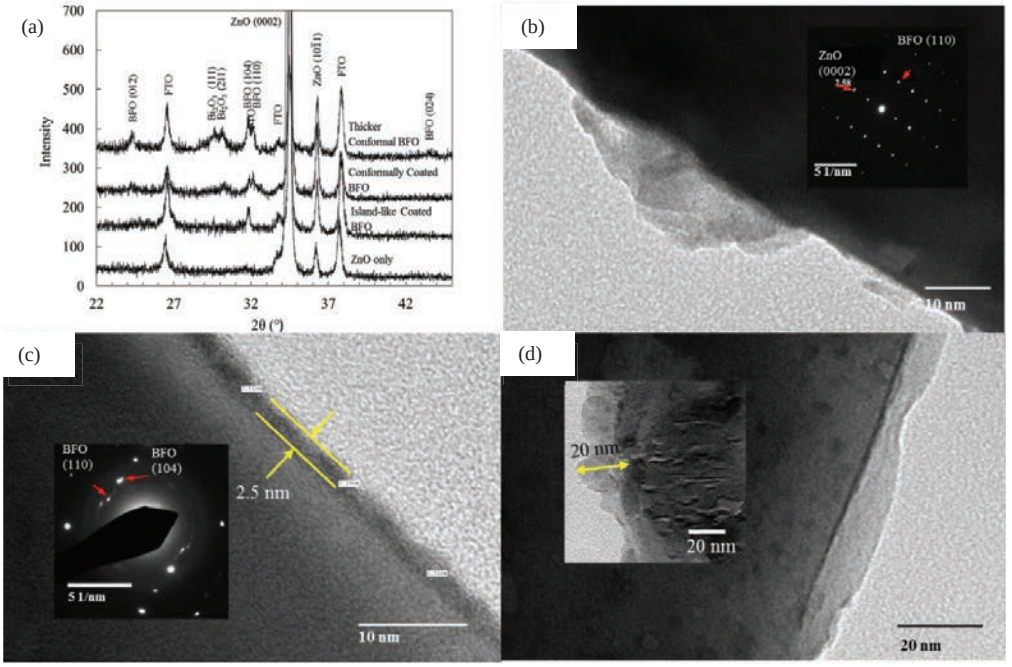

Fig. 2. ZnO-BFO nanorods. (a) X-ray diffraction patterns with varying BFO thicknesses, (b) TEM of island-like coated BFO (inset shows the SAED of the BFO coating) (c) TEM of conformal BFO coating (inset shows the SAED of the BFO coating) (d) TEM of thicker conformal BFO coating

The dominant BFO (110) and BFO (104) peaks shown in the SAED data were also confirmed in the XRD data.. When thicker BFO films were obtained, BFO (012) also started to appear, and also some secondary phases also started to appear. The presence of Bi_2O_3 were due to the 10 % excess $Bi(NO_3)_3.5H_2O$ to compensate for the loss of bismuth.

3.2. Solar Device Performance

The ZnO-BFO-N719-CuSCN (ZBNC) coated solar devices under 100 mW/cm^2 AM 1.5G illumination in Fig. 3 gave improved performances compared to ZnO-N719-CuSCN (ZNC) devices.[9,12] Table 2 provides a summary of results where the ZNC device had a J_{sc} of 0.64 mA/cm^2, V_{oc} of 0.38 V with an overall efficiency of 0.1 %. When BFO was added, the ZBNC V_{oc} values increased consistently to *ca* 0.5 V. The J_{sc} also increased to 0.79 mA/cm^2 with efficiencies of *ca* 0.2 % for the islands of BFO (I-ZBNC) device. When full conformal BFO coverage (C-ZBNC) was obtained at 0.15 M BFO sol, the J_{sc} increased significantly to a maximum J_{sc} of 1.4 mA/cm^2 with an efficiency of 0.38 %. On increasing the BFO sol to 0.3 M, thicker conformal coatings were obtained (T-ZBNC), and the J_{sc} showed a decrease to 0.81 mA/cm^2 with an efficiency drop to 0.24 %. Fill factors (FF) for all ZBNC devices were *ca* 0.55.

The IQE for the ZNC device had a maximum photoexcitation peak of *ca* 0.5 % due to the photoexcitation of ZnO as it occurred around the band gap of ZnO at the wavelength of *ca* 385 nm. The quantum efficiency dropped off quickly after 385 nm. A small broad “hump” *ca* 490 nm from the N719 dye indicated small influence of N719 dye on the charge injection outside the ZnO band structure. One of the problems faced by ZnO has been the issue of dye aggregation due to the formation of Zn^{2+} - dye complexes which resulted in charge recombination.[13] This has been linked to ZnO’s higher point of zero charge (pzc) at pH 9 compared to the optimal pH for dye sensitization at pH 5.[14] The formation of large amounts of dye aggregation in ZNC devices caused electron recombination before it could be transported through the N719 layer to ZnO.

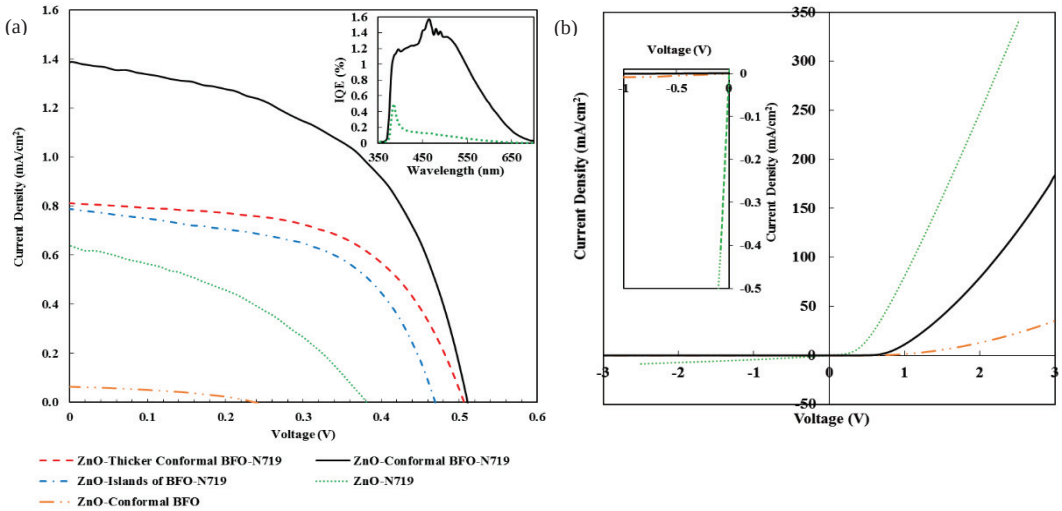

Fig. 3. (a) Comparison of current density-voltage of ZnO-based solar cells (inset shows the IQE of ZnO-conformal BFO–N719-CuSCN and ZnO-N719-CuSCN devices) under 100 mW/cm^2, 1.5AM illumination and (b) Dark current measurements of ZnO and ZnO-conformal BFO solar devices (inset shows magnified view of negative bias)

Table 2. . Performance of N719 sensitized ZnO solid state solar cells with varying BFO thickness

Device Structure	J_{sc} (mA/cm^2)	V_{oc} (V)	FF	η (%)	TOV (V)	RR
No BFO	0.64	0.38	0.39	0.10	0	35
Islands of BFO	0.79	0.47	0.56	0.20		
Conformal BFO	1.4	0.51	0.54	0.38	0.4	1064
Thicker Conformal BFO	0.81	0.51	0.57	0.24		
Conformal BFO w/o N719	0.063	0.24	0.40	0.006	0.4	66589

In contrast, the IQE for C-ZBNC solar cell exhibited a broad spread from *ca* 385 nm to *ca* 510 nm before a steep drop. It can be seen that the influence of N719 seen in the peaks between 485 – 510 nm were more significant compared to the ZNC devices. A maximum IQE of *ca* 1.6 % was also detected at the wavelength 465 nm, which was over 3 times the maximum IQE of the ZNC solar cell. The peak at 465 nm was indicative of the charge injection from BFO photoexcitation based on BFO's band gap of 2.7 eV.

The possibility of photovoltaic effect from BFO was explored, and ZnO-conformal BFO-CuSCN (C-ZBC) devices without N719 were fabricated to determine if BFO was an effective sensitizer. The J-V curve in Fig. 3(a) and performance results in Table 2 gave low J_{sc} values of 0.063 mA/cm^2 and efficiency of 0.006. This indicated that although BFO had photovoltaic effect, it did not act as a good sensitizer for ZnO. The improved performance thus had to be due to another reason.

The effect of dye aggregation for the BFO coated devices were studied and compared with the ZNC devices. The dye extracts from the various samples were compared using the absorbance data. The N719 exhibits metal-to-ligand charge transfer (MLCT) characteristics with an absorption band in the visible light range at 534 nm as well as another in the near UV range at 389 nm (inset of Fig. 4). The dye extracted from the ZNC device showed a blue shift to 497 nm and 365 nm due to an increase in the LUMO of the N719 ligands caused by the Zn^{2+} - dye complexes.[15] The MLCT of the dye extracted from the C-ZBNC device was detected at 510 nm and 365 nm, which is was closer to the MLCT for N719, implying there is less Zn^{2+} - dye complexes. This was confirmed when the amount of dye adsorbed using the Beer-Lambert law was determined. ZNC was higher at 1.01 x 10^{-7} mol cm^{-2} compared to 0.314 x 10^{-7} mol cm^{-2} for ZBNC devices; confirming the presence of less dye aggregates in the BFO coated devices. The reduction in dye aggregates occurred as the pzc of BFO is at pH 6.5,[16] which is closer to the optimal pH 5 for dye sensitization compared to ZnO. The reduction of Zn^{2+} - dye complexes reduced current recombination in the BFO coated devices.

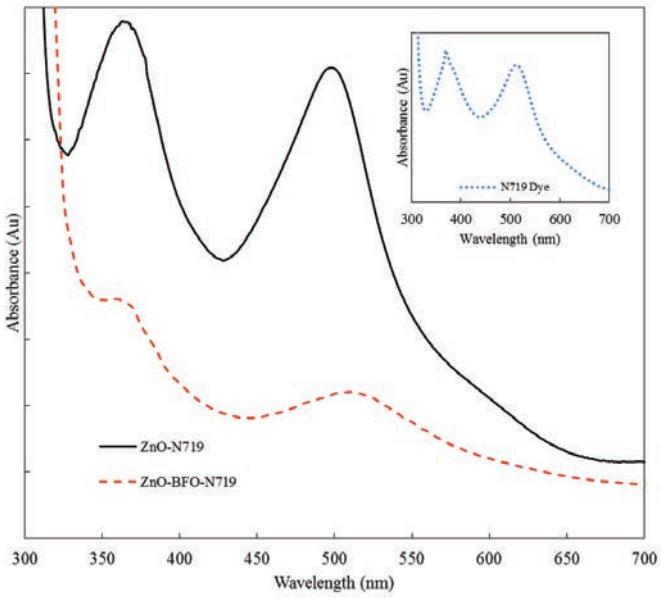

Fig. 4. Comparison of absorbance data for dye loading of ZnO and ZnO-BFO samples (inset shows absorbance data for N719 dye

As the J_{sc} of the ZBNC devices decreased with increased BFO thickness after reaching a peak at full conformal coverage; other mechanisms were also occurring besides the reduction in dye aggregation. ZNC devices were also plagued by current recombination due to the back flow of electrons from the ZnO conduction band to CuSCN or the dye.[17] The BFO electron affinity shown in Fig. 5 was slightly more positive than the electron affinity for N719. This band alignment allowed BFO to act as an electron blocking layer which prevents the back flow of electrons, thus decreasing current recombination.

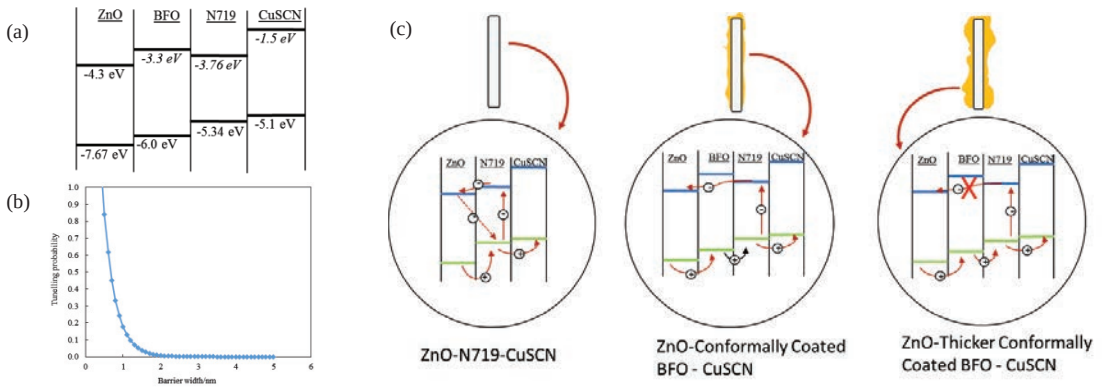

Fig. 5. Schematic representation of (a) Energy bands of ZBNC architecture, (b) Charge transport mechanisms of ZNC and ZBNC solar cells

The tunnelling probability was used to estimate the probability for an electron to tunnel though a square energy barrier.[18] The probability for tunneling plot showed that the BFO thickness had to be less than *ca* 2 nm for electrons to tunnel through the film. However, the 2 nm thickness is likely to be an underestimation, as BFO-ZnO forms a p-n junction which would further improve the carrier transfer. This puts it close to the 2.5 nm thick BFO film for the optimally performing ZBNC devices. Based on the probability shown, further increases in the BFO

thickness would decrease the number of carriers that can tunnel through, resulting in a drop in J_{sc} values for the T-ZBNC devices.

4. Conclusion

In conclusion, we have presented a method which allowed the deposition of low pH sol-gel layers on ZnO. The conformal BFO coating on ZnO nanorods was demonstrated to be able to enhance the performance of a solid state dye-sensitized solar cell by increasing the J_{sc} and V_{oc} and improving the device efficiency by a factor of 4. The improvements were due to several mechanisms. The BFO enabled a reduction of dye aggregation which reduced the current recombination occurring with Zn^{2+} - dye complexes. The BFO with N719 also acted as an electron blocking layer which prevented the back flow of electrons from recombining with the oxidized dye or CuSCN. These changes to the recombination and interface properties lead to the enhanced performance of the device. The enhancement can be further optimized when the BFO coating was controlled effectively to ensure conformal coverage and having a thickness of less than 2 nm to allow the electrons to tunnel through.

Acknowledgements

Funding from The Leverhulme Trust is acknowledged.

References

[1] L. Loh, S. Dunn, Recent Progress in ZnO-Based Nanostructured Ceramics in Solar Cell Applications, J. Nanosci. Nanotechnol. 12 (2012) 8215–8230.
[2] H.J. Snaith, Perovskites: The Emergence of a New Era for Low-Cost, High-Efficiency Solar Cells, J. Phys. Chem. Lett. 4 (2013) 3623–3630.
[3] M. Liu, M.B. Johnston, H.J. Snaith, Efficient planar heterojunction perovskite solar cells by vapour deposition, Nature. 501 (2013) 395+.
[4] S.R. Basu, L.W. Martin, Y.H. Chu, M. Gajek, R. Ramesh, R.C. Rai, et al., Photoconductivity in BiFeO(3) thin films, Appl. Phys. Lett. 92 (2008) 91905.
[5] M.D.L. Olvera, A. Maldonado, R. Asomoza, M. Melendez-Lira, Chemical stability of doped ZnO thin films, J. Mater. Sci. Electron. 11 (2000) 1–5.
[6] J. Briscoe, D.E. Gallardo, S. Hatch, V. Lesnyak, N. Gaponik, S. Dunn, Enhanced quantum dot deposition on ZnO nanorods for photovoltaics through layer-by-layer processing, J. Mater. Chem. 21 (2011) 2517–2523.
[7] S.M. Hatch, J. Briscoe, S. Dunn, A Self-Powered ZnO-Nanorod/CuSCN UV Photodetector Exhibiting Rapid Response, Adv. Mater. 25 (2013) 867–871.
[8] S.M. Hatch, J. Briscoe, S. Dunn, Improved CuSCN–ZnO diode performance with spray deposited CuSCN, Thin Solid Films. 531 (2013) 404–407.
[9] L. Loh, J. Briscoe, S. Dunn, Perovskite enhanced solid state ZnO solar cells, J. Phys. Conf. Ser. 476 (2013) 012008.
[10] C. Tso, C. Zhung, Y. Shih, Y.-M. Tseng, S. Wu, R. Doong, Stability of metal oxide nanoparticles in aqueous solutions., Water Sci. Technol. 61 (2010) 127–33.
[11] L. Loh, J. Briscoe, S. Dunn, Chemical Protection of ZnO Nanorods at Ultralow pH To Form a Hierarchical BiFeO 3 /ZnO Core–Shell Structure, ACS Appl. Mater. Interfaces. 7 (2015) 152–157.
[12] L. Loh, J. Briscoe, S. Dunn, Enhanced performance with bismuth ferrite perovskite in ZnO nanorod solid state solar cells, Nanoscale. 6 (2014) 7072–7078.
[13] H. Horiuchi, R. Katoh, K. Hara, M. Yanagida, S. Murata, H. Arakawa, et al., Electron injection efficiency from excited N3 into nanocrystalline ZnO films: Effect of (N3-Zn2+) aggregate formation, J. Phys. Chem. B. 107 (2003) 2570–2574.
[14] M. Kosmulski, The pH-dependent surface charging and the points of zero charge, J. Colloid Interface Sci. 253 (2002) 77–87.
[15] K. Keis, E. Magnusson, H. Lindstrom, S.E. Lindquist, A. Hagfeldt, A 5% efficient photo electrochemical solar cell based on nanostructured ZnO electrodes, Sol. Energy Mater. Sol. Cells. 73 (2002) 51–58.
[16] S. Iakovlev, C.H. Solterbeck, M. Kuhnke, M. Es-Souni, Multiferroic BiFeO3 thin films processed via chemical solution deposition: Structural and electrical characterization, J. Appl. Phys. 97 (2005).
[17] B.C. O'Regan, F. Lenzmann, Charge transport and recombination in a nanoscale interpenetrating network of n-type and p-type semiconductors: Transient photocurrent and photovoltage studies of TiO2/Dye/CuSCN photovoltaic cells, J. Phys. Chem. B. 108 (2004) 4342–4350.
[18] S.M. Sze, Physics of Semiconductor Devices, 3rd ed., Wiley-Interscience, New York, 2007.